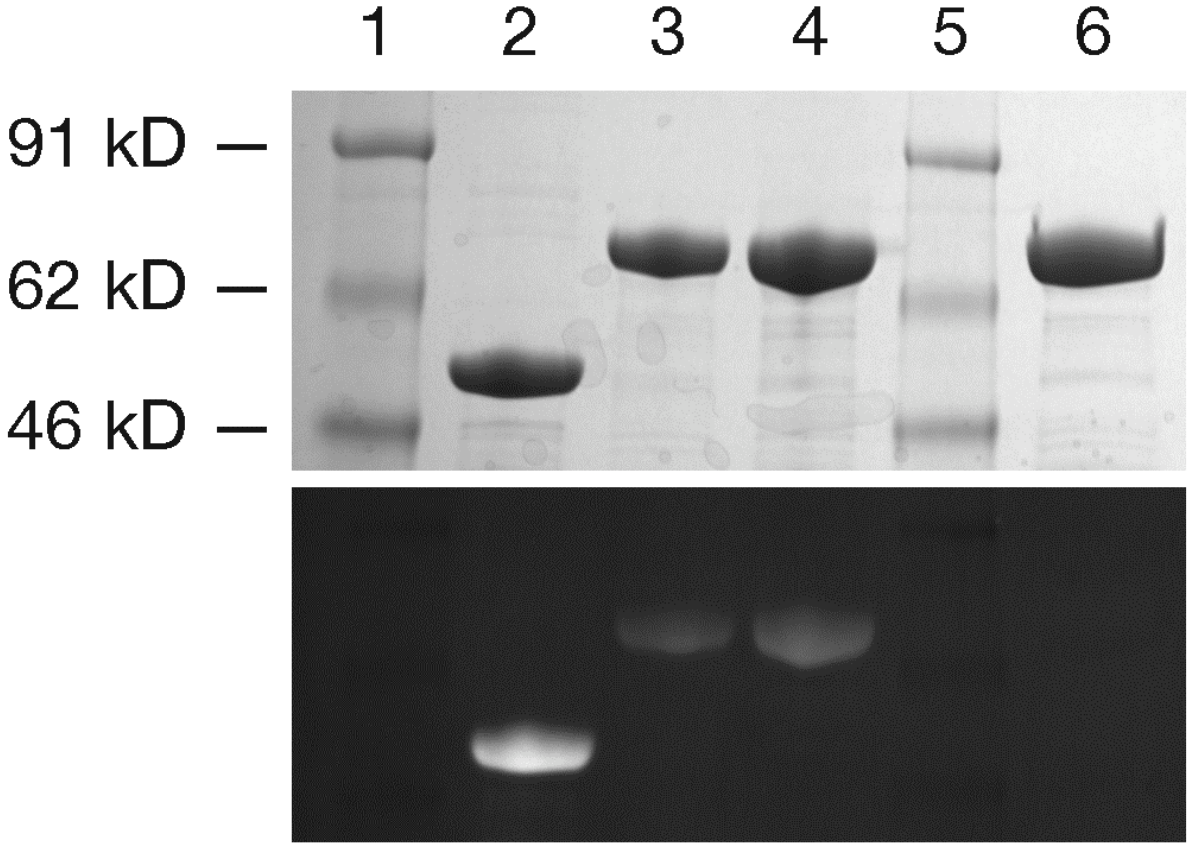

Supplemental Figure 1: Purification of Tlr0924. Both proteins were expressed in *E. coli* with C-terminal His_6 tags with concomitant synthesis of PCB (*1*) as described in the Methods. Purified proteins were characterized by SDS-PAGE with visualization by Coomassie Blue (top) or zinc blot (bottom). Lanes are 1, molecular weight standards; 2, holoCph1-N514 (positive control, (*2*)); 3, wildtype Tlr0924; 4, C_{499}D Tlr0924; 5, molecular weight standards; 6, C_{527}A Tlr0924.

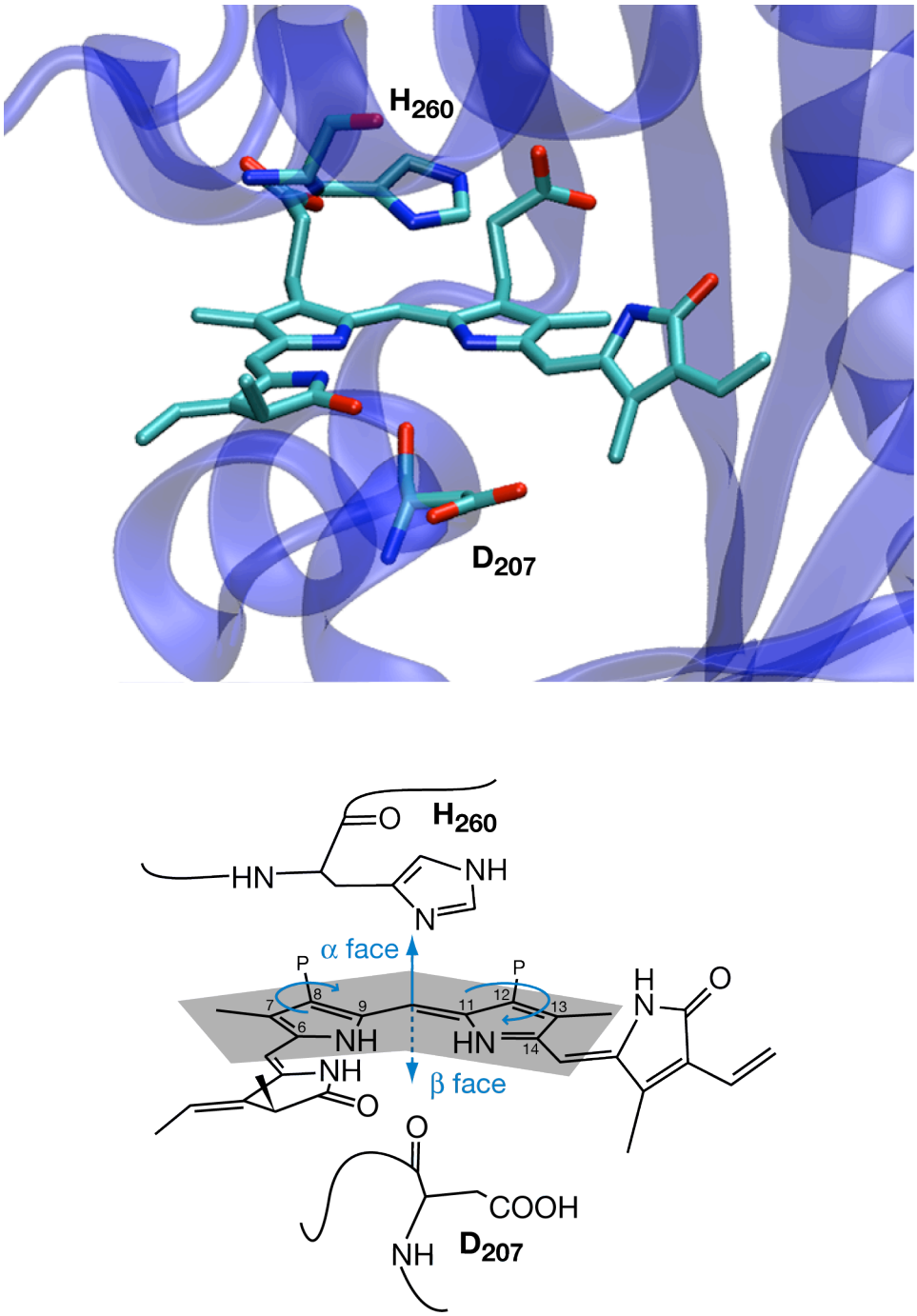

Supplemental Figure 2: Ring-facial definition for bilin adducts of biliproteins. Top, the bilin chromophore of *Dr*BphP (*3*) is shown with the A ring on the left and with His260 "above" and Asp207 "below" the plane of the B and C rings. Bottom, the same residues are shown in cartoon format. The atoms in the grey polygon are approximately coplanar. The *Z,syn* configuration at C10 implies that the face definitions of Rose and coworkers (*4*) for the B and C rings will be the same, as is shown in blue. The α face permits the ring numbering to be followed in a clockwise manner. P, propionate.

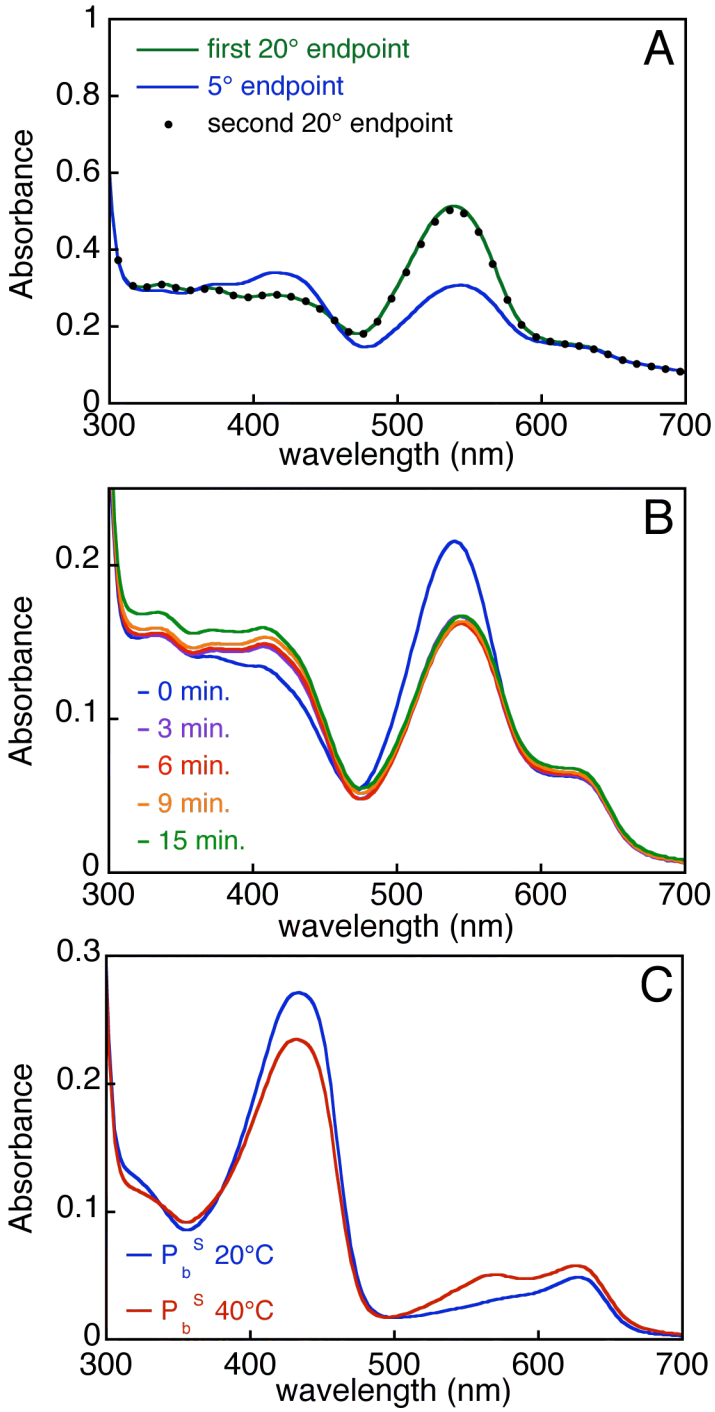

Supplemental Figure 3: The P_b^L and P_g' states of Tlr0924. (a) Absorbance spectra for Tlr0924 at thermal equilibrium in the P_g state at 20°C (green), 5°C (blue), and after return to 20°C (black dotted). (b) Tlr0924 was cycled to the P_g state at 40°C and then cooled to 5°C to accumulate P_b^L. The sample was then irradiated with blue light, and spectra were taken at the indicated times. (c) Tlr0924 was cycled from P_g to P_b^S by irradiation with green light at different temperatures. Spectra are shown for P_b^S at 20°C (solid) and 40°C (dashed).

Alignment 1:

```
Tlr0924         -----RLKTSLEREMIVSTIIQDIRQSIRLEEILQRAVNSIQQLLLSDRVLIYRFLGDGS
DrBphP          LEFEPTEAWDSTGPHALRNAMFALESAPNLRALAEVATQTVRELTGFDRVMLYKFAPDAT
                         .      : . :  :..: .*. : : *.::::::   ***::*:*  *.:

Tlr0924         GIVAVEATTLPQYSILGQVIHDPCFTKETARRFLEGRTLSISDVNQAQL-----------
DrBphP          GEVIAEARREGLHAFLGHRFPASDIPAQARALYTRHLLRLTADTRAAAVPLDPVLNPQTN
                * * .**     :::**: :  . :. ::   : .      :*.. * :

Tlr0924         -------------QDCYRELLTRLQVQANLVVPLLQGQHLWGLLIAHHCRSPRLWQREEL
DrBphP          APTPLGGAVLRATSPMHMQYLRNMGVGSSLSVSVVVGGQLWGLIACHHQT-PYVLPPDLR
                             .  : : * .: * :.* *.:: * :****: .**   * :   :

Tlr0924         FLLQRIAEPLTVALQQAEMYE
DrBphP          TTLESLGRLLSLQVQVKEA--
                  *: :.. *:: :*  *
```

Alignment 2:

```
Tlr0924         -----RLKTSLEREMIVSTIIQDIRQSIRLEEILQRAVNSIQQLLLSDRVLIYRFLGDGS
DrBphP          LEFEPTEAWDSTGPHALRNAMFALESAPNLRALAEVATQTVRELTGFDRVMLYKFAPDAT
                         .      : . :  :..: .*. : : *.::::::   ***::*:*  *.:

Tlr0924         GIVAVEATTLPQYSILGQ--VIHDPCFTKETARRFLEGRTLSISDVNQAQL---------
DrBphP          GEVIAEARREGLHAFLGHRFPASD--IPAQARALYTRHLLRLTADTRAAAVPLDPVLNPQ
                * * .**     :::**:     *  :. ::   : .      :*.. * :

Tlr0924         ---------------QDCYRELLTRLQVQANLVVPLLQGQHLWGLLIAHHCRSPRLWQRE
DrBphP          TNAPTPLGGAVLRATSPMHMQYLRNMGVGSSLSVSVVVGGQLWGLIACHHQT-PYVLPPD
                             .  : : * .: * :.* *.:: * :****: .**   * :   :

Tlr0924         ELFLLQRIAEPLTVALQQAEMYE
DrBphP          LRTTLESLGRLLSLQVQVKEA--
                    *: :.. *:: :*  *
```

Supplemental Figure 4: Alignments used in homology modeling of the Tlr0924 GAF domain. Sequence alignments of the Tlr0924 GAF domain (amino acids 421-592) and the GAF domain of DrBphP (amino acids 124-321) are shown. Top, alignment of Cys499 of Tlr0924 with Asp207 of DrBphP was predicted by several alignment packages, including CLUSTAL and MUSCLE (*5-8*). As discussed in the text, the resulting model caused steric clashes upon docking of bilin chromophore. We therefore generated a second alignment (bottom) manually to treat the region around Cys499 as an insertion loop in the homology modeling step. This approach aligned Asp497 of Tlr0924 (conserved in class II cyanobacteriochromes: Supp. Fig. 8) with Asp207 of DrBphP, which is conserved in phytochromes. The DIP motif of DrBphP and the DXCF motif of Tlr0924 are shown in bold.

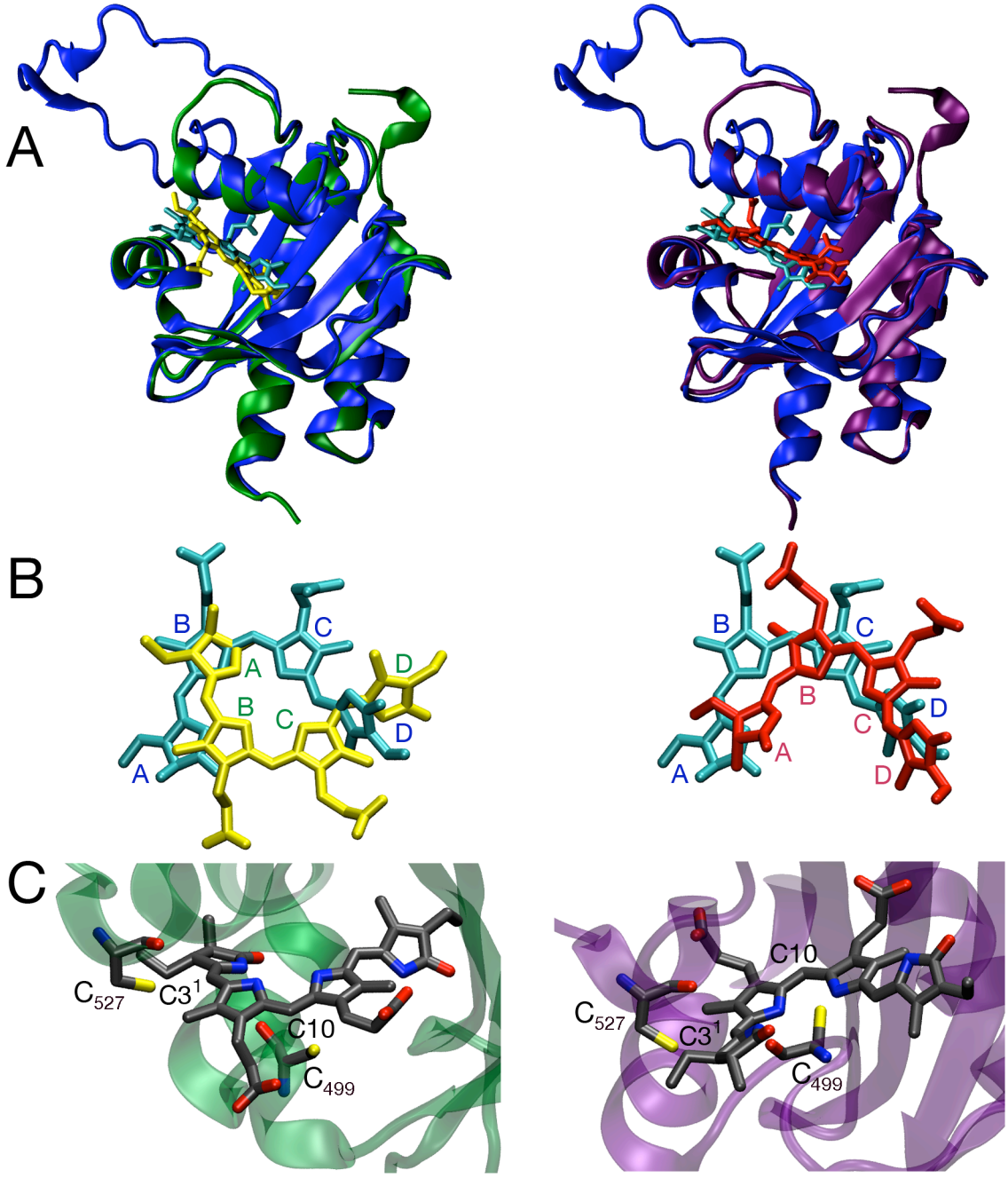

Supplemental Figure 5: Sequence alignments between *Dr*BphP and Tlr0924 (Supp. Fig. 4) were used to prepare homology models of the Tlr0924 GAF domain. PCB chromophore was docked in either a "flipped" orientation (left) or a "standard" orientation (right). (a) The overall fold of the models (purple, "standard;" green, "flipped") is compared to that of *Dr*BphP (blue). Bilin chromophores are shown (*Dr*BphP, cyan; "standard," red; "flipped," yellow). (b) The orientation of bilin in the two models is compared to that of *Dr*BphP. Color codes are as in (a). (c) The location of PCB chromophore relative to Cys527 and Cys499 is shown. In both models, Cys527 is well positioned for reaction with the $C3^1$ carbon, while Cys499 is well positioned in proximity to the C10 methine bridge.

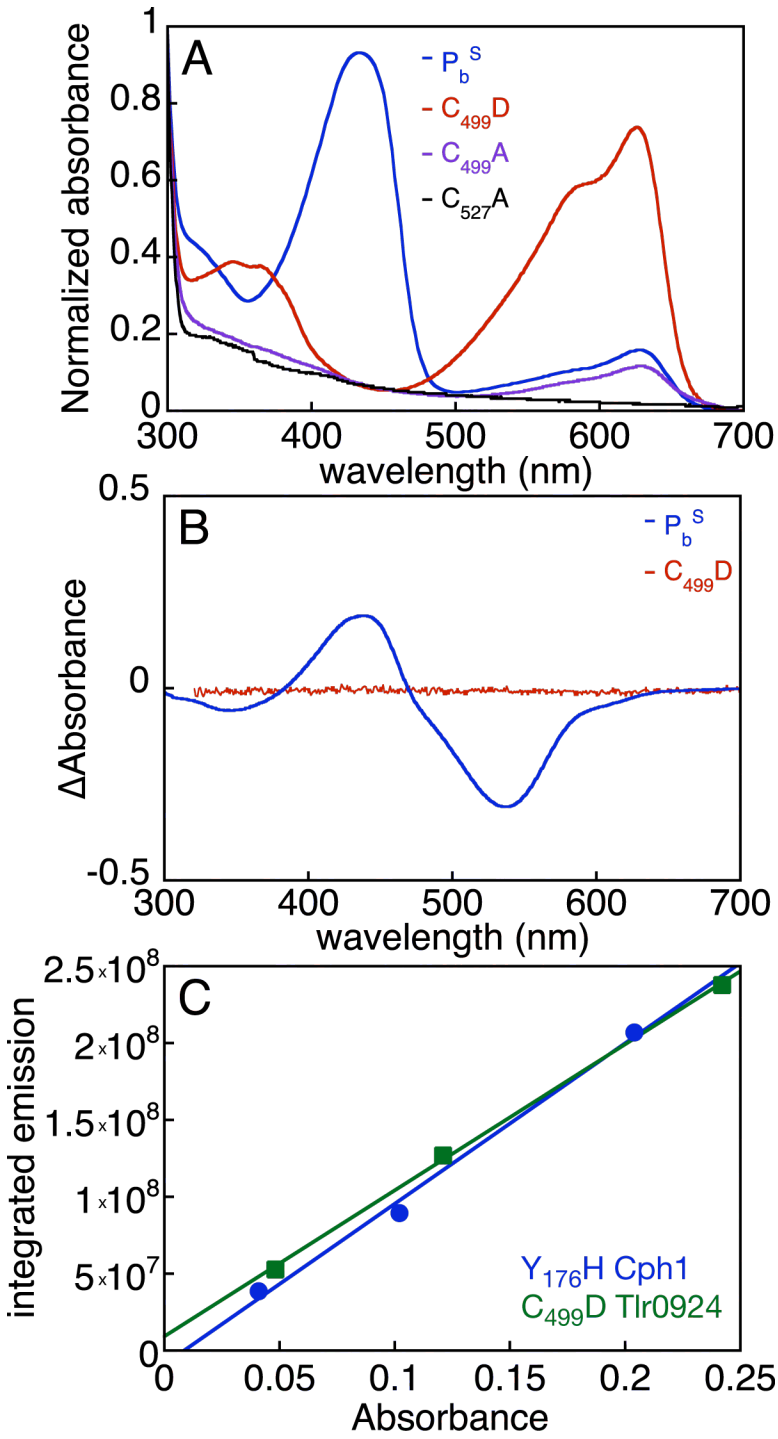

Supplemental Figure 6: Further characterization of $C_{499}D$ Tlr0924. (a) Absorbance spectra (normalized for the protein absorbance band) are shown for wildtype Tlr0924 (P_b^S state, blue), $C_{499}D$ Tlr0924 (red), $C_{499}A$ (purple) and $C_{527}A$ (black). (b) The photochemical difference spectra at room temperature are shown for wildtype (blue) and $C_{499}D$ (red) Tlr0924. (c) Fluorescence emission is plotted against peak absorbance for dilution series of $Y_{176}H$ Cph1 (blue) and $C_{499}D$ Tlr0924 (green).

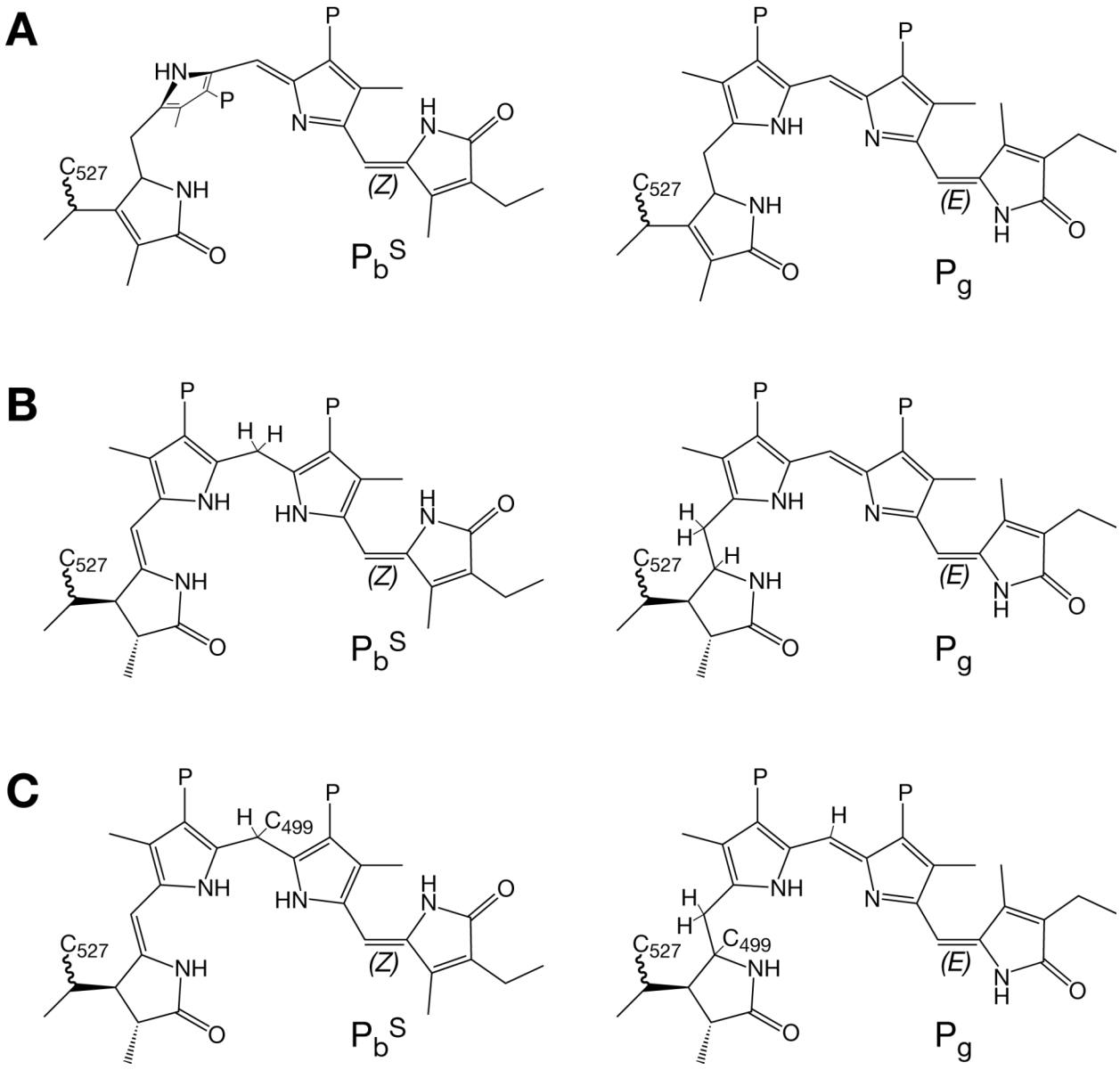

Supplemental Figure 7: Alternative models for the blue/green photocycle of Tlr0924. (a) The 2-state model proposed by Ikeuchi and colleagues (*9*) postulates a *15Z* PVB chromophore with the B-ring twisted out of conjugation (which would correspond to P_b^S). Photoconversion to *15E* destabilizes this twisted structure, resulting in P_g. This model is inconsistent with the CD spectrum of P_b^S (see Discussion). (b) P_b^S could arise from reduction of C10 to yield phycocyanorubin. Tautomerization to 2,3-dihydrophycoviolobilin would yield P_g. (c) The proposed second linkage between Cys499 and C10 (Figure 7) could itself migrate to C4, resulting in a 2,3-dihydro-4-cysteinyl-phycoviolobilin P_g state. P, propionate.

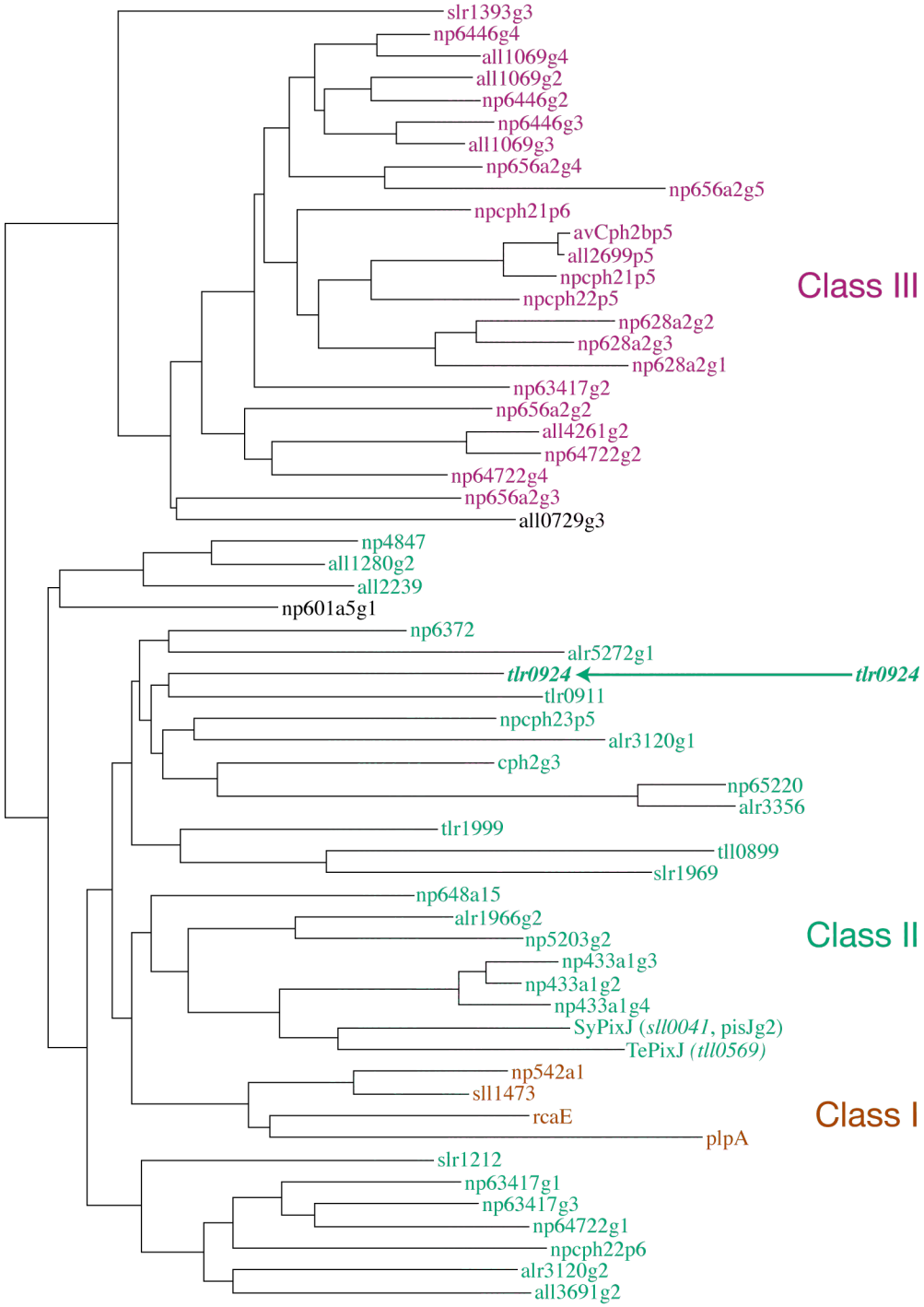

Supplemental Figure 8: Preliminary phylogeny of cyanobacteriochrome GAF domains. An alignment of 59 Phr GAF domains was prepared using MUSCLE (*5*, *6*), and a phylogenetic tree was prepared from the resulting alignment using CLUSTAL (*8*). Sequence names are color-coded by the sequence aligned with the PXXDIP motif of phytochromes: class I Phr proteins, XXEVFP (orange); class II Phr proteins or cyanobacteriochromes, XDXCFX (green); class III Phr proteins, XXD(Y/H)LQ (magenta). Tlr0924 is indicated.

Supplemental Table 1: Dihedral angles for TDDFT calculations

C5 configuration	A ring	D ring	C4/5	C5/6	C9/10	C10/11	C14/15	C15/16
Z, syn[a]	α_f	α_f	+3.3	+15.9	-9.6	-11.5	-151.6	+5.5
Z, syn	α_f	β_f	+5.3	+21.1	-9.9	-8.6	+151.8	-3.6
Z, syn	β_f	α_f	-5.4	-21.3	+9.1	+8.1	-148.4	+3.1
Z, syn	β_f	β_f	-6.6	-18.7	+9.7	+11.8	+149.0	-4.6
Z, anti	α_f	α_f	-5.1	+145.8	-10.2	-13.1	-147.5	+5.1
Z, anti[b]	α_f	β_f	-6.0	+142.7	-13.0	-11.7	+150.1	-5.5
Z, anti	β_f	α_f	+1.7	-145.1	-12.2	-13.4	-145.7	+4.8
Z, anti	β_f	β_f	+3.9	-142.0	-12.7	-10.8	+146.1	-6.5

All TDDFT calculations were performed in the gas phase on a model compound mimicking the PCB adduct of Cph1 but replacing the thioether linkage to C3[1] with a proton and replacing the propionate side chains with methyl groups. Dihedral angles are reported about each methine bridge for the final B3LYP/6-31+G* geometries used for TDDFT. Geometry optimizations were performed in GAMESS or Q-Chem (*10, 11*). Dihedral angles are defined starting with the adjacent nitrogen as the highest-priority substituent. Thus, the C4/5 dihedral is defined as N_A-C4-C5-C6, while the C5/6 dihedral is defined as N_B-C6-C5-C4. All values are in degrees.

[a]This configuration corresponds to the P_r state of *Dr*BphP.

[b]This configuration corresponds to α-PC.

REFERENCES FOR SUPPLEMENTARY MATERIAL

(1) Gambetta, G. A., and Lagarias, J. C. (2001) Genetic engineering of phytochrome biosynthesis in bacteria. *Proc. Natl. Acad. Sci. U. S. A. 98*, 10566-10571.

(2) Fischer, A. J., and Lagarias, J. C. (2004) Harnessing phytochrome's glowing potential. *Proc. Natl. Acad. Sci. U. S. A. 101*, 17334-17339.

(3) Wagner, J. R., Zhang, J., Brunzelle, J. S., Vierstra, R. D., and Forest, K. T. (2007) High resolution structure of *Deinococcus* bacteriophytochrome yields new insights into phytochrome architecture and evolution. *J. Biol. Chem. 282*, 12298-12309.

(4) Rose, I. A., Hanson, K. R., Wilkinson, K. D., and Wimmer, M. J. (1980) A suggestion for naming faces of ring compounds. *Proc. Natl. Acad. Sci. U. S. A. 77*, 2439-2441.

(5) Edgar, R. C. (2004) MUSCLE: a multiple sequence alignment method with reduced time and space complexity. *BMC Bioinform. 5*, 113.

(6) Edgar, R. C. (2004) MUSCLE: multiple sequence alignment with high accuracy and high throughput. *Nucl. Acids Res. 32*, 1792-1797.

(7) Higgins, D. G., Thompson, J. D., and Gibson, T. J. (1996) Using CLUSTAL for multiple sequence alignments. *Meth. Enzymol. 266*, 383-402.

(8) Thompson, J. D., Higgins, D. G., and Gibson, T. J. (1994) CLUSTAL W: improving the sensitivity of progressive multiple sequence alignment through sequence weighting, position-specific gap penalties and weight matrix choice. *Nucl. Acids Res. 22*, 4673-4680.

(9) Ishizuka, T., Narikawa, R., Kohchi, T., Katayama, M., and Ikeuchi, M. (2007) Cyanobacteriochrome TePixJ of Thermosynechococcus elongatus harbors phycoviolobilin as a chromophore. *Plant Cell Physiol. 48*, 1385-1390.

(10) Schmidt, M. W., Baldridge, K. K., Boatz, J. A., Elbert, S. T., Gordon, M. S., Jensen, J. H., Koseki, S., Matsunaga, N., Nguyen, K. A., Su, S., Windus, T. L., Dupuis, M., Montgomery, J. A. Jnr. (1993) General atomic and molecular electronic structure system. *J. Comput. Chem. 14*, 1347-1363.

(11) Shao, Y., Molnar, L. F., Jung, Y., Kussmann, J., Ochsenfeld, C., Brown, S. T., Gilbert, A. T., Slipchenko, L. V., Levchenko, S. V., O'Neill, D. P., DiStasio, R. A., Jr., Lochan, R. C., Wang, T., Beran, G. J., Besley, N. A., Herbert, J. M., Lin, C. Y., Van Voorhis, T., Chien, S. H., Sodt, A., Steele, R. P., Rassolov, V. A., Maslen, P. E., Korambath, P. P., Adamson, R. D., Austin, B., Baker, J., Byrd, E. F., Dachsel, H., Doerksen, R. J., Dreuw, A., Dunietz, B. D., Dutoi, A. D., Furlani, T. R., Gwaltney, S. R., Heyden, A., Hirata, S., Hsu, C. P., Kedziora, G., Khalliulin, R. Z., Klunzinger, P., Lee, A. M., Lee, M. S., Liang, W., Lotan, I., Nair, N., Peters, B., Proynov, E. I., Pieniazek, P. A., Rhee, Y. M., Ritchie, J., Rosta, E., Sherrill, C. D., Simmonett, A. C., Subotnik, J. E., Woodcock, H. L., 3rd, Zhang, W., Bell, A. T., Chakraborty, A. K., Chipman, D. M., Keil, F. J., Warshel, A., Hehre, W. J., Schaefer, H. F., 3rd, Kong, J., Krylov, A. I., Gill, P. M., and Head-Gordon, M. (2006) Advances in methods and algorithms in a modern quantum chemistry program package. *Phys. Chem. Chem. Phys. 8*, 3172-3191.